RSC Advances

PAPER

View Article Online
View Journal | View Issue

Cite this: *RSC Adv.*, 2021, **11**, 21781

Transition metal oxide (NiO, CuO, ZnO)-doped calcium oxide catalysts derived from eggshells for the transesterification of refined waste cooking oil

Nur Fatin Sulaiman,[ab] Nurul Izzaty Ramly,[a] Mohamad Helmi Abd Mubin[c] and Siew Ling Lee *[ab]

This paper reports the synthesis of new transition metal oxide-modified CaO catalysts derived from eggshells for the transesterification of refined waste cooking oil. CaO is a well-known base catalyst for transesterification. However, its moderate basicity and low surface area have restricted its catalytic performance. Therefore, a new attempt was made to modify the CaO catalyst with transition metal oxides, including Ni, Cu and Zn oxides, *via* simple wetness impregnation method. The catalytic performance of the resulting modified CaO-based catalysts was evaluated through the transesterification reaction using refined waste cooking oil. The results showed that the NiO/CaO(10 : 90)(ES) catalyst calcined at 700 °C, demonstrated being highly potential as a catalyst. It gave the highest biodiesel production (97.3%) at the optimum conditions of 1 : 18 oil-to-methanol molar ratio, 6 wt% catalyst loading and 180 minutes reaction time as verified by response surface methodology (RSM). The high catalytic activity of NiO/CaO(10 : 90)(ES)(700 °C) was attributed to its high basicity (8.5867 mmol g^{-1}) and relatively large surface area (7.1 m^2 g^{-1}). The acid value and free fatty acids of the biodiesel produced under optimal process conditions followed the EN 14214 and ASTM D6751 limit with 0.17 mg KOH per g (AV) and 0.09 mg KOH per g (FFA), respectively.

Received 16th March 2021
Accepted 2nd June 2021

DOI: 10.1039/d1ra02076e

rsc.li/rsc-advances

1. Introduction

Researchers are seeing new solutions to replace the reliance on petroleum fuel through increasing environmental concerns and the fastest depletion of fossil fuel in the world. In search of renewable sources as the replacement, biodiesel was introduced as a substitute source to fossil fuels. Since biodiesel has very similar physico-chemical properties to petroleum diesel, no engine modification is needed when biodiesel became the substitution. Biodiesel is a green fuel based on fats and plant oils that can be used in diesel engine. In addition, biodiesel has been recognized as a clean renewable and sustainable fuel that produces 78% less gaseous pollutant emission, such as SO_x, NO_x, CO and HC, and particulate matter or soot than petrol diesel.[1,2] The application of biodiesel as a renewable fuel does not increase the atmospheric carbon dioxide as most feedstocks used in biodiesel production are environmentally friendly.

The possibility of using vegetables oils and their derivatives is recognized as a substitute fuel for replacing petroleum diesel. In spite of that, the direct utilization of plant oils in a petroleum diesel engine was found to be impractical without a modification process due to the high viscosity of the oil possibly damaging the vehicle's engine. Undergoing a transesterification reaction is the most favourable method for decreasing oil's viscosity and producing biodiesel fuel.[3] However, replacing fossil fuels with vegetable oil leads to a high cost of biodiesel for its commercialization. Therefore, the idea of using waste vegetable oil, which is commonly known as waste cooking oil, has been introduced in the biodiesel production due to its low cost and gives a waste management solution.[4] In addition, it is possible to avoid the sensitive "food *versus* fuel" debate by using refined waste cooking oil for the production of biodiesel.[5]

Generally, biodiesel is known as a long chain fatty acid alkyl ester (FAAE) synthesized from the transesterification reaction of vegetable oil with alcohol in the presence of a catalyst. A homogeneous catalyst is a base catalyst from alkali metal methoxides and hydroxides, such as $NaOCH_3$, KOH and NaOH,[6] while a heterogeneous catalyst comes from alkali earth oxides, such as CaO, MgO, SrO and BaO, alkali metal oxide, supported alkali metal and zeolite.[2,7] In fact, homogeneous catalysts have some drawbacks, including the difficulty of separating the catalyst from the reaction mixture, high water consumption for washing the catalyst residues, and the formation of soap as an unwanted product.[2,8] Therefore, heterogeneous catalysts are now more popular. Unlike the homogenous catalyst, these

[a]*Department of Chemistry, Faculty of Science, Universiti Teknologi Malaysia, 81310 Johor Bahru, Malaysia. E-mail: nurfatinsulaiman@gmail.com; nurulizzaty438@yahoo.com; lsling@utm.my**

[b]*Centre for Sustainable Nanomaterials, Ibnu Sina Institute for Scientific and Industrial Research, Universiti Teknologi Malaysia, 81310 Johor Bahru, Malaysia*

[c]*Centre for Pre University Studies, MAHSA University, Bandar Saujana Putra, 42610 Jenjarom, Selangor, Malaysia. E-mail: mohamadhelmi@mahsa.edu.my*

heterogeneous catalysts could be easily recovered from the reaction mixture and possibly reusable for several times.

Calcium oxide (CaO) is the most promising heterogeneous base catalyst for the development of biodiesel because of the benefits, such as its low solubility in methanol, cheaper price, low toxicity, and it is not harmful to the environment. In addition, calcium sources for preparing the CaO catalyst can easily be obtained from a waste shell, like chicken eggshell, cockle shell, mussel shell, river snail shell and golden apple snails shell.[9,10] As studied by Kaewdaeng *et al.*,[11] the CaO derived from waste shell was demonstrated as a good heterogeneous catalyst in the biodiesel production because it gave higher catalytic activity, as well as being environmentally friendly in the production process. Moreover, the heterogeneous catalyst can be modified either by incorporation with an alkaline metal, alkaline earth metal and transition metal oxides *via* co-precipitation, sol–gel, hydration dehydration and chemical vapor deposition.

Despite the fact that CaO is a well-known catalyst for biodiesel production, the single CaO catalyst was reported to be not stable under certain reaction conditions. Moreover, CaO has a low surface area, which restricts the number of active basic sites on the catalyst surface, and it sometimes suffered from the leaching of Ca species during the transesterification process.[12] As a result, the catalytic performance of CaO in producing the maximum biodiesel yield was greatly affected. Therefore, many efforts have been made to modify the CaO catalyst in an attempt to improve the physicochemical properties of the CaO catalyst, including its catalytic activity, stability and basic strength.[13] This improvement in the physicochemical properties significantly affected the efficiency of biodiesel production. Doping with selective elements such as copper oxide would increase the basicity, surface area and reduce the particle size of the based catalyst. As explained by Yoo *et al.*,[14] the ZnO-based metal oxides were good basic solid catalysts for the transesterification of vegetable oils upon modification using alkaline or alkaline earth metals. Moreover, nickel oxide (NiO) has received considerable attention in different fields due to its significant catalytic, optical, electrical and magnetic properties.[15]

This study presents a new attempt to improve the catalytic performance of CaO derived from eggshell by transition metal doping *via* a simple wetness impregnation method. The main purpose of developing these mixed metal oxide catalysts was to enhance their physicochemical properties in terms of the stability, catalytic activity and basic strength of the catalysts. According to Gayakhe *et al.*,[16] transition metal oxides (such as NiO, CuO and ZnO) tend to become a co-catalyst because of their characteristics, including variable oxidation state, ion complex formation and high catalytic efficiency. To our best knowledge, the synthesis of the new mixed metal oxides by incorporation of transition metal oxides (NiO, CuO and ZnO) into calcium oxide-based catalysts derived from waste eggshells in the transesterification of refined waste cooking oil has not been explored. For this purpose, the effect of catalyst preparation parameters (such as calcination temperatures, types of dopants and ratios of dopant loading) was investigated in order produce an efficient catalyst for biodiesel production.

Moreover, the catalytic performance of the transition metal-doped CaO catalyst was further improved by varying the catalyst loading, reaction time and oil-to-methanol ratio. The catalytic results were verified using response surface methodology (RSM) coupled with Box–Behnken Design (BBD) to achieve the optimum biodiesel production parameters. Toward this objective, a linear or square polynomial function was employed to describe the experimental design, and thus to explore the modeling for the optimization.

2. Materials and methods

2.1. Chemicals and materials

Refined waste cooking oil has been collected from the local market. For catalyst production, waste chicken eggshells were collected from a seafood restaurant in Kulai, Johor. Chemicals, such as zinc nitrate hexahydrate ($Zn(NO_3)_2 \cdot 6H_2O$), nickel(II) nitrate hexahydrate ($Ni(NO_3)_2 \cdot 6H_2O$) and copper(II) nitrate trihydrate ($Cu(NO_3)_2 \cdot 3H_2O$), were acquired from Merck. Methanol (CH_3OH) as the reactant and *n*-hexane as the solvent were used for the transesterification process.

2.2. Synthesis of the calcium oxide-based catalyst

Waste chicken eggshells were rinsed with distilled water to remove dust and impurities. The shells were then dried overnight at a temperature of 105 °C. After drying, the shells were grounded into powder and calcined at 900 °C by heating at a ramping rate of 5 °C min^{-1} for 5 hours to obtain the CaO catalyst.[17] Next, the modification of the CaO-based catalyst with the addition of transition metal oxides as dopants was achieved using the wetness impregnation method. About 5 g of prepared CaO derived from waste chicken eggshells was dissolved into 50 mL of distilled water. Transition metals (nickel(II) nitrate hexahydrate, copper(II) nitrate trihydrate and zinc nitrate hexahydrate) as dopants were prepared by dissolved an appropriate amount of the salt solution into a based catalyst solution, according to the ratios 10 : 90, 20 : 80, 30 : 70 wt%, as stated in Table 1. Both solutions were then mixed into a beaker under stirring at room temperature for activation. After 30 minutes, the mixture was filtered and aged in the oven for 24 hours at 90 °C before the calcination process at 700, 800 or 900 °C for 5 hours.

Table 1 Preparation of the modified calcium oxide-based catalysts by doping transition metal oxides (NiO, CuO, ZnO) at different dopant-to-based ratios

Catalysts	Dopant-to-based ratios (wt%)
NiO/CaO(ES)	10 : 90
	20 : 80
	30 : 70
CuO/CaO(ES)	10 : 90
	20 : 80
	30 : 70
ZnO/CaO(ES)	10 : 90
	20 : 80
	30 : 70

2.3. Determination of the acid value (AV) and free fatty acid (FFA)

The analyses of refined waste cooking oil, especially acid value and free fatty acid, were carried out before the transesterification reaction in order to identify the properties of the feedstock. Thus, a simple titration method was carried out in accordance with the American Society for Testing Materials (ASTM D6751) and European Standard (EN 14214). A sample of about 5.00 g of refined waste cooking oil was placed in a dried conical flask. Then, 25 mL of ethanol was added with 2 to 3 drops of phenolphthalein. The mixture solution was heated and stirred for 10 minutes. The solution was titrated with 0.1 N KOH until the pink color appeared. The acid value was calculated using eqn (1), where A.V. is the acid value in (mg KOH per g), mL is the amount of potassium hydroxide (KOH) consumed by the sample, N is the normality of KOH and W is the weight of the oil in grams, while the FFA value was calculated using eqn (2):

$$\text{A.V.} = \frac{\text{mL} \times N \times 56.1}{W} \quad (1)$$

$$\text{FFA} = \frac{\text{A.V.}}{2.19} \quad (2)$$

2.4. Catalyst characterization

The characterization techniques used to identify the effect of physicochemical characteristics on the catalytic activity in transesterification for biodiesel were nitrogen adsorption–desorption analysis, X-ray diffraction spectroscopy (XRD), CO_2-temperature programmed desorption (CO_2-TPD), field emission scanning electron microscopy (FESEM) and energy dispersive X-ray (EDX) analyses. Nitrogen adsorption–desorption analysis was used for the measurement of the textural properties for the prepared catalyst by Micromeritics ASAP 2010. About 0.5 g of sample was degassed at 120 °C to remove the adsorbed gases. The specific surface area was determined from the adsorption curve in accordance with the Brunauer–Emmett–Teller (BET) method. For XRD study, the sample was placed in a glass plate of 10–15 mm diameter and approximately 1 mm depth in the sample holder. The XRD patterns were obtained using Cu-Kα radiation (λ = 1.54060 Å) for 2θ values from 20° to 80° by a Diffractometer D5000 Siemens Crystalloflex. The crystallite size of the prepared catalysts was determined by Scherrer's equation.

The surface morphology of the samples was examined *via* FESEM (Hitachi SU8020) coupled with an EDX analyzer. The prepared samples were coated with gold before the analysis, as the samples could be exposed to electron bombardment without any charging effect. CO_2-TPD analysis was carried out utilizing Micromeritics Autochem 2920. About 0.05 g of the sample was placed in a quartz U-tube of 10 mm internal diameter, and cleaned for 1 hour under helium flow for 20 mL min^{-1} at 150 °C. Next, the temperature was decreased to 40 °C for 1 hour to flow the CO_2 gas continuously through the sample in order to pre-saturate the active sites with CO_2. Finally, the helium gas was flowed at 80 °C for 1 hour to remove the weak physisorbed CO_2 from the surface of the samples.

2.5. Transesterification reaction for biodiesel production

For this process, refined waste cooking oil was refluxed at 65 ± 5 °C with methanol in the presence of the prepared catalyst. Next, the methanol removal process was continued by distillation process. The product was then centrifuged at 5000 rpm for 10 minutes in order to separate the used catalyst from the solution. Two layers consisting of the top layer (biodiesel) and bottom layer (catalyst and glycerol) were formed. Further analysis of the biodiesel product was carried out using a gas chromatography-flame ionization detector (GC Agilent 6890N model) equipped with a DB-HeavyWAX (30 m × 0.255 mm × 0.25 μm). The oven temperature was set at 250 °C, while the injector and detector temperatures were fixed at 250 °C. The initial column temperature was programmed at 60 °C for 2 minutes with a ramp rate of 5 °C min^{-1} up to 240 °C for 7 minutes. Helium was used as a carrier gas. A sample of 10 : 1 ratio (n-hexane to biodiesel) was injected from the diluted biodiesel. Biodiesel production was calculated using eqn (3), in accordance with EN 14103:2011.

$$Y = \frac{\sum A - A_{\text{EI}}}{A_{\text{EI}}} \times \frac{W_{\text{EI}}}{W} \times 100 \quad (3)$$

where $\sum A$ is the total peak area from the methyl ester in C6 : 0 to that in C24 : 1. A_{EI} is the peak area corresponding to nanodecanoic acid methyl ester, while W_{EI} is the weight (mg) of the nanodecanoic acid methyl ester being used as an internal standard and W is the weight (mg) of the sample.

2.6. Optimization parameters of the transesterification reaction

The effect of the reaction parameters, including the catalyst loadings with respect to the oil weight (2, 4, 6 and 8 wt%), oil-to-methanol mol ratios (1 : 16, 1 : 18, and 1 : 20) and the reaction times (30, 60, 120, 180 and 240 minutes), was studied over the best performing modified CaO-based catalyst. The reusability of the used prepared catalyst was examined in multiple cycles.

2.7. Regression model and statistical analysis

In order to verify the statistical experimental design and then achieve the best model equation, the biodiesel production parameters were generated and validated using the Response Surface Model (RSM) given by the Design-Expert 7.1.6. The design is a polynomial empirical model in the second order, and describes the response surface (eqn (4)).

$$Y = \beta_0 + \Sigma\beta_i X_i + \Sigma\beta_{ii} X_i^2 + \Sigma\beta_{ij} X_i X_j + \varepsilon \quad (4)$$

where Y is the response, β_0, β_i, β_{ii} and β_{ij} are the coefficients for the intercept, linear, square and interaction effect, respectively, while X_i and X_j are designated as the independent factors and ε represents the error detected in the response Y.

There were three identified independent factors, including catalyst loading (X_1), oil-to-methanol ratio (X_2) and reaction time (X_3), while the percentage of the biodiesel yield was selected as the response (Y). Independent factors were calculated for the maximum response for biodiesel production, ranging from low to high levels codified as −1, 0, and +1. A Box–Behnken design (BBD), with a total of 17 experiments randomized to reduce errors from orderly factors patterns,

Table 2 The Box–Behnken design of the independent factors on the transesterification reaction

No.	Independent factors		
Run order	X_1: catalyst loading (wt%)	X_2: oil-to-methanol ratio (mol ratio)	X_3: reaction time (min)
1	8	1 : 18	240
2	4	1 : 20	180
3	6	1 : 18	180
4	4	1 : 18	120
5	8	1 : 18	120
6	8	1 : 20	180
7	6	1 : 18	180
8	6	1 : 18	180
9	6	1 : 18	180
10	8	1 : 16	180
11	6	1 : 20	120
12	6	1 : 20	240
13	4	1 : 18	240
14	6	1 : 16	120
15	6	1 : 18	180
16	6	1 : 16	240
17	4	1 : 16	180

followed the second order surface response model. Table 2 presents the independent factors-coded level BBD. In the analysis of variance (ANOVA), the validity for response to the model was generated. The significant design must be referred to as the *F*-value (Fischer variation ratio) and *p*-value (significant probability value), in which the *p*-value of the selected design must be less than 0.05 and insignificant due to lack of fit. In addition, the determination coefficient (R^2) must be >0.94, indicating the right correlation between the experiment and the predicted values. The relationship between the two independent factors were examined using 2D contour plots and 3D response surface plots, while the third factor remained constant.

3. Results and discussion

3.1. Catalytic testing

The catalytic performances on the transesterification reaction of refined waste cooking oil using different transition metal oxides (NiO, CuO, ZnO)-impregnated calcium oxide-based catalysts derived from waste chicken eggshells were investigated under the following reaction conditions: 65 °C reaction temperature, 6 wt% catalyst loading, 1 : 18 oil-to-methanol mol ratio and 60 min reaction time. The effects of different synthesis parameters, including calcination temperatures, types of dopants and dopant-to-based ratios, were studied and optimized to obtain the highest catalytic activity for the modified CaO-based catalysts in the production of biodiesel.

3.1.1. Effect on the types of dopants. The biodiesel production over the NiO/CaO (ES), CuO/CaO (ES) and ZnO/CaO (ES) catalysts with a 10 : 90 wt% dopant-to-based ratio calcined at different temperatures of 700, 800 and 900 °C are presented in Fig. 1. It was observed that at a temperature of 700 °C, the NiO/CaO(10 : 90)(ES) catalyst showed the highest biodiesel production of 97.30%, followed by the ZnO/CaO(10 : 90)(ES) catalyst (96.38%) and CuO/CaO(10 : 90)(ES) catalyst (94.93%). Moreover, at 800 °C, the higher biodiesel production of 96.46% was obtained using the NiO/CaO(10 : 90)(ES) catalyst. Overall, it was found that the addition of the NiO species led to the highest biodiesel production in the transesterification reaction of refined waste cooking oil compared to CuO and ZnO. As mentioned by Dawood *et al.*,[15] nickel oxide has received considerable attention as a good heterogeneous catalyst due to its high surface area and possible porous nature.

3.1.2. Effect on the calcination temperatures. Fig. 2 shows the effect of the calcination temperature over the NiO/CaO (ES), CuO/CaO (ES) and ZnO/CaO (ES) catalysts with a 10 : 90 wt% dopant-to-based ratio towards the percentage of biodiesel production. For the NiO/CaO(10 : 90)(ES) catalyst, its catalytic activity decreased with increasing temperature from 700 °C (97.30%) to 900 °C (90.55%). This phenomenon was mainly due

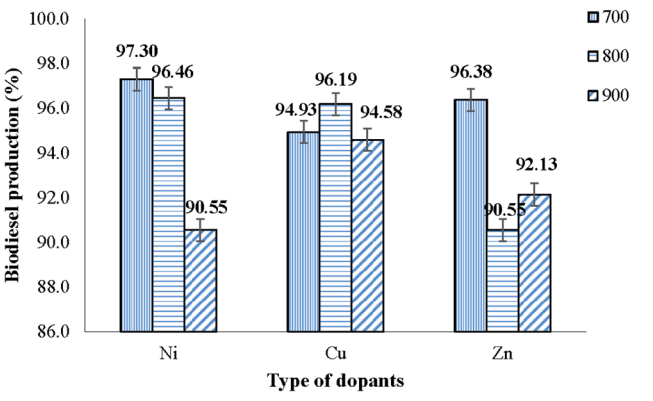

Fig. 1 Percentage of biodiesel production over the NiO/CaO (ES), CuO/CaO (ES) and ZnO/CaO (ES) catalysts with 10 : 90 wt% dopant-to-based ratio calcined at different calcination temperatures for 5 hours.

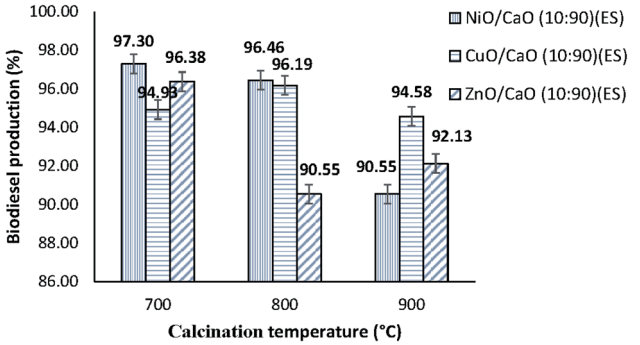

Fig. 2 Percentage of biodiesel production over NiO/CaO(10 : 90)(ES), CuO/CaO(10 : 90)(ES) and ZnO/CaO(10 : 90)(ES) calcined at 700, 800 and 900 °C for 5 hours.

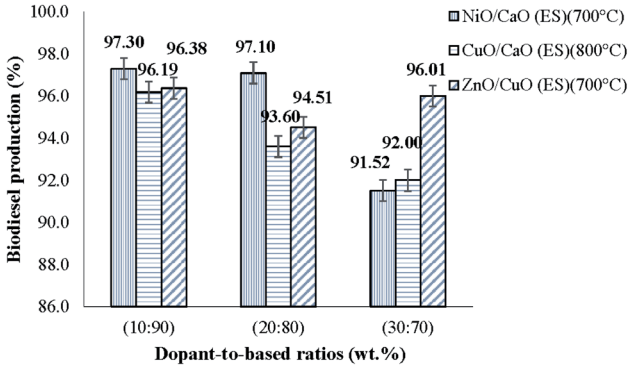

Fig. 3 Percentage of biodiesel production over the NiO/CaO (ES), ZnO/CaO (ES) catalysts calcined at 700 °C and CuO/CaO (ES) catalyst calcined at 800 °C for 5 hours with different dopant-to-based ratios (10 : 90, 20 : 80, 30 : 70 wt%).

to the sintering effect and recrystallization of the metal oxide, resulting in low dispersion of the catalysts and poor catalytic materials.[18]

Meanwhile, the catalytic performance of the CuO/CaO(10 : 90)(ES)(700 °C) catalyst had resulted in 94.93% of biodiesel yield since the catalyst particles were agglomerated, as shown in Fig. 6(c), and subsequently reduced the active species on the catalyst surface. Interestingly, the catalytic performance increased significantly to 96.19% of biodiesel production for the CuO/CaO(10 : 90)(ES) catalyst calcined at 800 °C. However, the biodiesel percentage was reduced to 94.58% upon increasing the calcination temperature to 900 °C. It was believed that the reduction was due to the sintering effect, where the solid catalyst has undergone the process of compacting and forming a solid mass of material by heating at high temperature, and hence led to an increase in the particle size and decrease in the surface area. For the ZnO/CaO(10 : 90)(ES) catalyst calcined at 700 °C, a higher percentage biodiesel production was achieved at 96.38%.

As shown in Fig. 2, the current findings revealed that the optimum calcination temperature for NiO/CaO(10 : 90)(ES) (97.30%), ZnO/CaO(10 : 90)(ES) (96.38%) and CuO/CaO(10 : 90)(ES) (96.19%) catalysts were 700 °C, 700 °C and 800 °C, respectively. These modified catalysts prepared at the optimum calcination temperature were used to further study the effect of dopant loading towards catalytic activity. As suggested by Yan *et al.*,[19] the calcination temperature was a critical aspect in controlling the surface defects and the interaction between the metal oxides. Moreover, the catalytic activity and thermal stability of the catalyst increased with the addition of an appropriate amount of dopant due to the high dispersion of the metal on the catalyst.[20]

3.1.3. Effect on the dopant loadings. The effects of the dopant loadings on the transesterification process for biodiesel over the NiO/CaO (ES) and ZnO/CaO (ES) catalysts calcined at 700 °C and the CuO/CaO (ES) catalyst calcined at 800 °C were investigated with modifying the dopant-to-based ratios for 10 : 90, 20 : 80 and 30 : 70 wt%, as illustrated in Fig. 3. For the NiO/CaO (ES)(700 °C) catalyst, the highest biodiesel production (97.30%) was obtained when the dopant-to-based ratio used was 10 : 90 wt%. However, the catalytic activity was reduced with increasing Ni loadings to 20 wt% (97.10%) and 30 wt% (91.52%). As stated by Sulaiman *et al.*,[21] excessive dopant loading caused agglomeration on the catalyst surface, blocking pores and the number of active sites. A similar trend was observed for the CuO/CaO (ES)(800 °C) and ZnO/CaO (ES)(700 °C) catalysts when the optimum dopant-to-based ratio was 10 : 90 wt%, exhibiting 96.19% and 96.38%, respectively, for the biodiesel production.

3.2. Properties of the refined waste cooking oil and biodiesel product

The physicochemical fuel properties of the refined waste cooking oil and biodiesel produced over the NiO/CaO(10 : 90)(ES) catalyst calcined at 700 °C were calculated in accordance with the American Society for Testing Materials (ASTM D6751) and European Standard (EN 14214), as listed in Table 3. The density of the refined waste cooking oil was higher (950 kg m^{-3}) compared with the biodiesel produced (870.6 kg m^{-3}) due to the changes in the chemical properties, where the triglycerides undergo several processes to form the fatty acid methyl ester. Moreover, the viscosity of the biodiesel produced at 40 °C was 4.9 $mm^2 s^{-1}$, which is in accordance with the range specified by ASTM D6751 and EN 14214. The high viscosity recorded for the refined waste cooking oil (20.8 $mm^2 s^{-1}$) causes poor flow of the fuel in the engine combustion chamber during the intake stroke. This causes it to take a long time to mix with air, and thus delays the combustion.

The acid value for refined waste cooking oil was 0.39 mg KOH per g, which is well within the range of both standards and suitable for the transesterification of oil. After the reaction, the acid values of the biodiesel product over the NiO/CaO(10 : 90)(ES)(700 °C) catalyzed reaction were reduced to 0.17 mg KOH per g. Overall, the findings for the AV and FFA under optimal process conditions met the standard value of ASTM D6751 and EN 14214. Hence, the refined waste cooking oil employed in this study seems to have the capability for large-scale biodiesel production with a suitable catalyst.

3.3. Catalyst characterizations

3.3.1. Nitrogen adsorption–desorption analysis. The surface area and porosity of four different transition metal-

Table 3 Physicochemical fuel properties of refined waste cooking oil and biodiesel produced using the NiO/CaO(10 : 90)(ES)(700 °C) catalyst

Parameter	Test method	EN 14214	ASTM D6751	Refined waste cooking oil	Biodiesel (FAME)
Acid value (mg KOH per g)	EN 14104	Max. 0.5	Max. 0.8	0.39	0.17
Free fatty acid (mg KOH per g)	EN 14104	Max. 0.25	Max. 0.4	0.20	0.09
Density at 15 °C (kg m^{-3})	ASTM D1298	860–890	860–890	950	870.6
Kinematic viscosity at 40 °C (mm^2 s^{-1})	ASTM D445	3.5–5.0	1.9–6.0	20.8	4.9

Table 4 Textural properties of the NiO/CaO(10 : 90)(ES) catalyst calcined at 700 °C and 800 °C, and the CuO/CaO(10 : 90)(ES) and ZnO/CaO(10 : 90)(ES) catalysts calcined at 700 °C for 5 hours

Catalysts	Calcination temperature (°C)	BET surface area (m^2 g^{-1})	Average pore diameter (nm)	Total pore volume (cm^3 g^{-1})
NiO/CaO(10 : 90)(ES)	700	7.1	14.26	0.0135
	800	5.7	17.68	0.0110
CuO/CaO(10 : 90)(ES)	700	7.0	14.27	0.0130
ZnO/CaO(10 : 90)(ES)	700	5.6	17.86	0.0101

modified catalysts of NiO/CaO(10 : 90)(ES) calcined at 700 °C and 800 °C, CuO/CaO(10 : 90)(ES)(700 °C) and ZnO/CaO(10 : 90)(ES)(700 °C) were measured *via* nitrogen adsorption–desorption analysis. As presented in Table 4, the BET surface area of the NiO/CaO(10 : 90)(ES) catalyst was affected by calcination temperature. It was observed that the surface area of the NiO/CaO(10 : 90)(ES) catalyst reduced from 7.1 m^2 g^{-1} to 5.7 m^2 g^{-1} as the calcination temperature increased from 700 °C to 800 °C. Meanwhile, the pore volume also decreased from 0.0135 cm^3 g^{-1} (700 °C) to 0.0110 cm^3 g^{-1} (800 °C) with an increase in the calcination temperature. The decrease in the surface area and pore volume at higher calcination temperature was possibly due to the structural modification of the catalyst, whereby the catalyst particles began to agglomerate.[22] In contrast, the pore diameter of the catalyst increased from 14.26 to 17.68 nm by increasing the calcination temperature from 700 to 800 °C.

On the other hand, the BET surface area, average pore diameter and pore volume recorded by the CuO/CaO(10 : 90)(ES) catalyst calcined at 700 °C were 7.0 m^2 g^{-1}, 14.27 nm and 0.0130 cm^3 g^{-1}, respectively. Meanwhile, for the ZnO/CaO(10 : 90)(ES) catalyst, the surface area, average pore diameter and pore volume were 5.6 m^2 g^{-1}, 17.86 nm and 0.0101 cm^3 g^{-1}, respectively. Although the overall structural properties possessed by the modified catalysts did not show a significant difference, the NiO/CaO(10 : 90)(ES) catalyst calcined at 700 °C exhibited the largest value of surface area and pore volume, as well as achieved a maximum biodiesel production of 97.30%. As mentioned by Dawood *et al.*,[15] NiO has attracted extensive interest as a good heterogeneous catalyst because of its large specific surface area and possible porous nature.

Meanwhile, the pore size distribution curves of the series of modified catalysts, NiO/CaO(10 : 90)(ES) calcined at 700 °C and 800 °C, CuO/CaO(10 : 90)(ES)(700 °C) and ZnO/CaO(10 : 90)(ES)(700 °C), are represented in Fig. 4. The results showed that the pattern of all series of modified catalysts illustrated relatively broad pore size distributions with a pore size of less than 50 nm, signifying a mesoporous structure. According to Melero *et al.*,[23] the mesopores of the solid catalyst are significant to minimize the diffusional constraints of bulky free fatty acid molecules and long alkyl chain molecules. Obviously, the NiO/CaO(10 : 90)(ES) catalyst calcined at 700 °C presented a higher pore volume and smaller pore diameter compared to the others. This finding is in close alliance with Ljupković *et al.*,[24] who demonstrated that the pore diameter and pore volume play an essential role in exhibiting the catalytic productivity.

3.3.2. X-ray diffraction (XRD) analysis. Fig. 5 displays the X-ray diffractograms of the NiO/CaO(10 : 90)(ES) catalyst calcined at 700 °C and 800 °C, and the CuO/CaO(10 : 90)(ES) and ZnO/CaO(10 : 90)(ES) catalysts calcined at 700 °C. As can be seen in Fig. 5, all modified catalysts exhibited intensive peaks of the

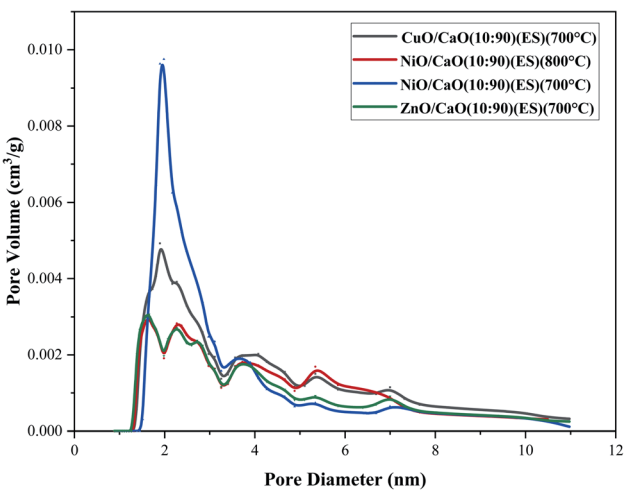

Fig. 4 Pore size distribution of the NiO/CaO(10 : 90)(ES) catalyst calcined at 700 °C and 800 °C, CuO/CaO(10 : 90)(ES) and ZnO/CaO(10 : 90)(ES) catalysts calcined at 700 °C.

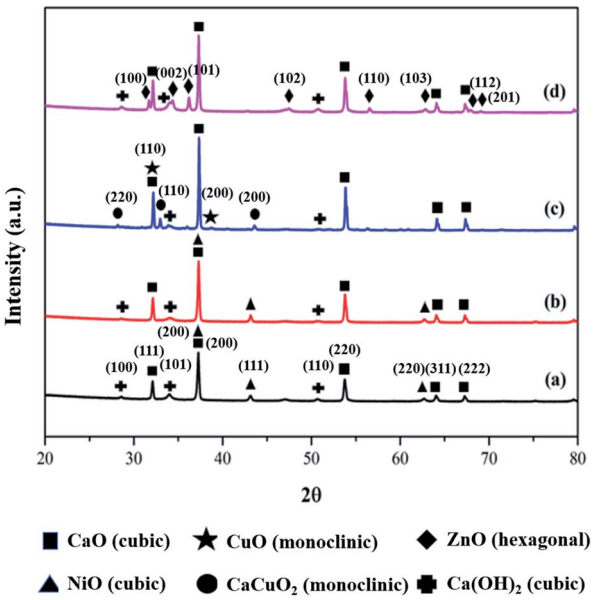

Fig. 5 XRD diffractograms of the catalysts: (a) NiO/CaO(10 : 90)(ES)(700 °C), (b) NiO/CaO(10 : 90)(ES)(800 °C), (c) CuO/CaO(10 : 90)(ES)(700 °C), and (d) ZnO/CaO(10 : 90)(ES)(700 °C).

CaO phases and crystallinity peaks of the transition metal oxide phases. The major peaks of the CaO cubic phase appeared at 2θ values approximately equal to 37.38° (I_{100}), 53.89° (I_{50}), 32.22° (I_{42}), 64.19° (I_{12}) and 67.42° (I_{11}) at plane *hkl* values of (200), (220), (111), (311) and (222), respectively, according to the JCPDS 77-2376 crystallographic file. Moreover, minor peaks of the hexagonal shape portlandite $Ca(OH)_2$ were detected for all of the modified catalysts at 2θ values equal to 34.17° (I_{100}), 50.91° (I_{31}) and 28.74° (I_{22}) attributed to *hkl* planes of (101), (110) and (100), respectively, according to JCPDS 44-1481. This trace impurity was probably due to the exposure of the catalyst with atmospheric air before analysis. The NiO/CaO(10 : 90)(ES) catalysts calcined at 700 °C and 800 °C showed similar patterns of XRD peaks, where the diffraction reflections assigned to the NiO cubic crystalline phase were observed at 2θ values equal to 43.25° (I_{100}), 37.23° (I_{64}) and 62.83° (I_{52}) attributed to the *hkl* planes of (111), (200) and (220), respectively, corresponding to JCPDS 73-1523. In addition, there was an overlapping peak between NiO cubic and CaO cubic at a 2θ value equal to 37.23° (I_{64}) at the *hkl* plane of (200).

For the CuO/CaO(10 : 90)(ES) catalyst calcined at 700 °C, there were three peaks assigned to the monoclinic CuO corresponding to JCPDS 89-2531. One peak was found at 2θ = 38.99° (I_2) at the *hkl* plane of (200). Another two peaks were overlapped with CaO cubic at 32.18° (I_{39}) and 67.33° (I_{11}) attributed to the *hkl* planes of (110) and (220), respectively. Moreover, the formation of new phases was detected referring to tetragonal $CaCuO_2$ at around 2θ = 32.82° (I_{33}), 28.03° (I_{15}) and 43.69° (I_4), which were attributed to the *hkl* planes of (110), (220) and (200), respectively, according to JCPDS 88-0568. This new phase formation was probably due to the large interaction between CuO and CaO, leading to the formation of the $CaCuO_2$ compound.

Meanwhile, the ZnO/CaO(10 : 90)(ES) catalyst calcined at 700 °C displayed the presence of a hexagonal ZnO peak at 2θ values of 36.26° (I_{100}), 31.77° (I_{58}), 34.42° (I_{42}), 56.60° (I_{32}), 62.86° (I_{29}), 47.54° (I_{22}), 67.95° (I_{24}) and 69.09° (I_{12}) attributed to the *hkl* planes of (101), (100) (002), (110), (103), (102), (112) and (201), respectively, corresponding to JCPDS 79-0206. The overall results had suggested that the Ni^{2+}, Cu^{2+} and Zn^{2+} cations from the transition metal oxides-doped CaO were not displaced into either the interstitial positions or the substitutional sites of the CaO crystal structure due to the coexistence of the transition metal oxides, and CaO peaks were observed in the XRD diffractogram. Therefore, the impregnation of 10 wt% transition metal oxides into the CaO (ES)-based catalyst was successfully done, as the formation of transition metal oxides and CaO were detected segregated by the XRD analysis.

Table 5 presents the crystallite sizes for the modified catalysts that were determined by Debye Scherer's equation. It was noted that the crystallite sizes of these catalysts were affected by the introduction of different transition metal oxides (NiO, CuO and ZnO) doped into the CaO (ES) catalyst. The smallest crystallite size was recorded for the NiO/CaO(10 : 90)(ES) catalyst calcined at 700 °C with 36.44 nm (CaO) and 28.27 nm (NiO). However, the crystallite sizes of CaO and NiO were slightly increased to 40.32 nm and 32.91 nm, respectively, as the calcination temperature was increased to 800 °C. According to Roy *et al.*,[25] a higher calcination temperature would promote cluster agglomeration and reduce the surface area. This statement is aligned with the BET surface area, which decreased with the increase of the calcination temperature. The crystallite size was inversely proportional to the BET surface area, in which a large crystallite size could reduce the surface area of the catalyst.[26]

Moreover, the CuO/CaO(10 : 90)(ES) catalyst calcined at 700 °C recorded the highest crystallite size of CaO (55.24 nm), CuO (41.91 nm) and $CaCuO_2$ (41.81 nm), followed by the crystallite size of the ZnO/CaO(10 : 90)(ES) catalyst calcined at

Table 5 Crystallite size of the NiO/CaO(10 : 90)(ES) catalysts prepared at calcination temperatures of 700 °C and 800 °C, and the CuO/CaO(10 : 90)(ES) and ZnO/CaO(10 : 90)(ES) catalysts prepared at a calcination temperature of 700 °C

		Crystallite size (nm)					
Catalyst	Calcination temperature (°C)	CaO	$Ca(OH)_2$	NiO	CuO	$CaCuO_2$	ZnO
Ni/CaO(10 : 90)(ES)	700	36.44	20.98	28.27	—	—	—
Ni/CaO(10 : 90)(ES)	800	40.32	16.39	32.91	—	—	—
Cu/CaO(10 : 90)(ES)	700	55.24	18.70	—	41.91	41.81	—
Zn/CaO(10 : 90)(ES)	700	43.93	16.30	—	—	—	34.09

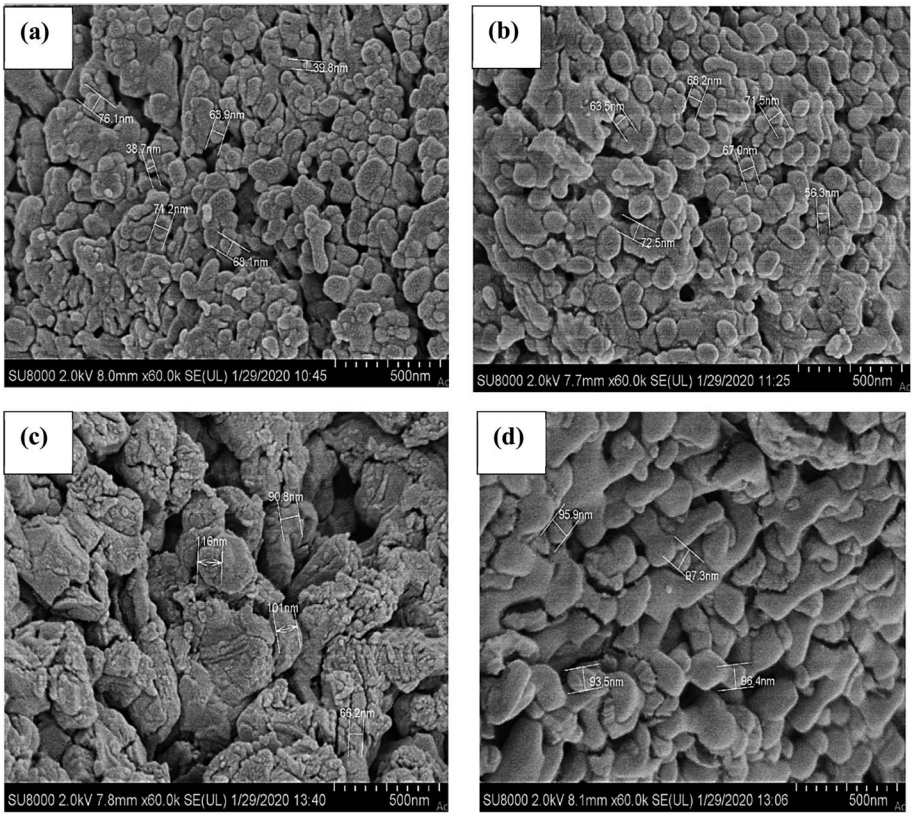

Fig. 6 FESEM micrographs of the catalysts: (a) NiO/CaO(10 : 90)(ES)(700 °C), (b) NiO/CaO(10 : 90)(ES)(800 °C), (c) CuO/CaO(10 : 90)(ES)(700 °C) and (d) ZnO/CaO(10 : 90)(ES)(700 °C) with a magnification of 60k×.

700 °C, which achieved 43.93 nm (CaO) and 34.09 nm (ZnO). The influences of these types of transition metal oxide catalysts toward the crystallite size of the CaO (ES) catalyst were observed in this study. It was found that the smallest crystallite size of CaO was 36.44 nm when doped with NiO, followed by ZnO (43.93 nm) and CuO (55.24 nm). As reported by Kamal *et al.*,[27] a larger crystallite size could lower the catalytic performance of the catalyst toward biodiesel production.

3.3.3. Field emission scanning electron microscopy (FESEM) analysis. Fig. 6 illustrates the FESEM micrographs of the NiO/CaO(10 : 90)(ES) catalysts calcined at 700 °C and 800 °C, and CuO/CaO(10 : 90)(ES) and ZnO/CaO(10 : 90)(ES) catalysts calcined at 700 °C captured at 60k× magnification. Overall, the micrographs showed an irregular shape with varied particle size on the surface of the catalysts. Based on the FESEM micrograph in Fig. 6(a), the NiO/CaO(10 : 90)(ES) catalyst calcined at 700 °C showed the formation of an irregular spherical shape with smaller particle sizes ranging from 38.70 nm to 74.20 nm. Certain particles are bonded together as aggregated with various grain sizes distributed on the catalyst surface. According to Niju *et al.*,[28] the smaller grain size could provide a greater surface area, which then enhanced the catalyst efficiency. However, when increasing the calcination temperature to 800 °C, the micrographs showed a slightly densely-packed structure with spherical size in the range of 56.30 nm to 72.50 nm distributed on the catalyst surface, as observed in Fig. 6(b). This morphology exhibited a less porous network and this is in accordance with the study by Sulaiman *et al.*,[29] which stated that the porosity of the catalyst decreases as the temperature increases. The smaller number of pores at higher heat treatment is probably due to the fracturing of the porous wall.

The morphology of the CuO/CaO(10 : 90)(ES) catalyst calcined at 700 °C shown in Fig. 6(c) exhibited uneven shapes with the agglomeration of particles. The agglomerated particles, which are larger with particle sizes ranging from 66.2 nm to 116.0 nm, possibly had blocked some pores of the catalyst surface. Thus, they hindered the access of the reactant to the active sites and decreased the catalytic activity. For the ZnO/CaO(10 : 90)(ES) catalyst calcined at 700 °C, the catalyst exhibited a mixture of irregular spherical and rod-shaped particles that bonded together, producing a densely-packed arrangement of crystallites, as observed in Fig. 6(d). The irregular-shaped particles with larger sizes of 93.5 nm to 97.3 nm were distributed on the catalyst's surface, forming an agglomerated structure.

3.3.4. Energy dispersive X-ray (EDX) analysis. Fig. 7 displays the results of EDX analysis for the NiO/CaO(10 : 90)(ES) catalysts calcined at 700 °C and 800 °C, and the CuO/CaO(10 : 90)(ES) and ZnO/CaO(10 : 90)(ES) catalysts calcined at 700 °C. It was found that all elements, including Ni, Cu, Zn, Ca and O, were present in the mixed metal oxide catalysts. These elements existed on the surface of the catalysts, and their elemental compositions confirmed the weight percentages. As can be seen, the composition of Ca was high over all of the

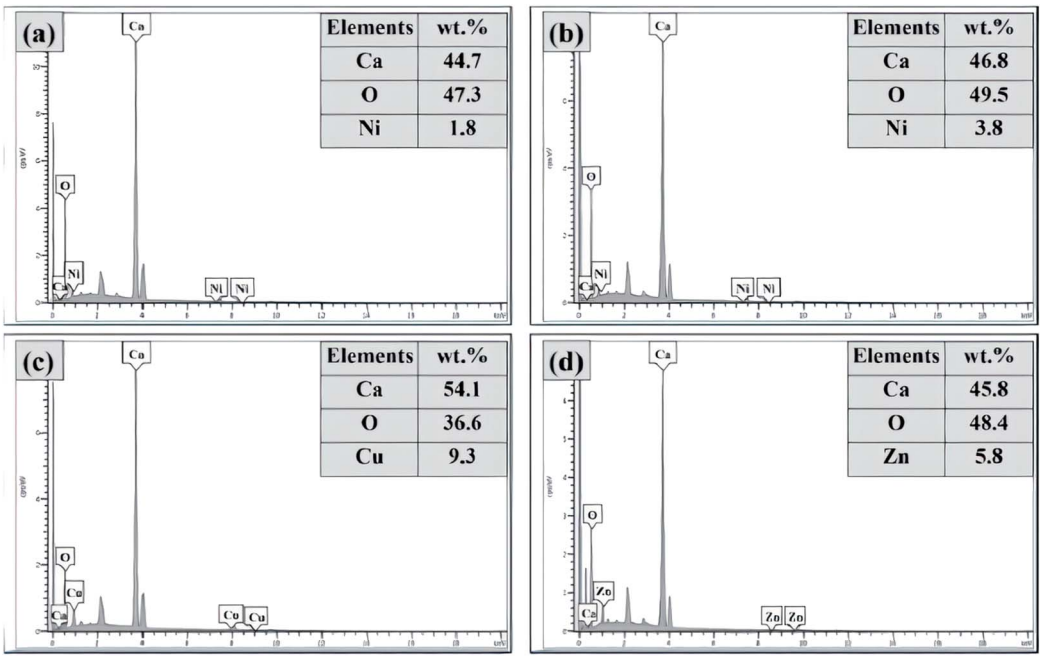

Fig. 7 Elemental compositions of the catalysts: (a) NiO/CaO(10 : 90)(ES)(700 °C), (b) NiO/CaO(10 : 90)(ES)(800 °C), (c) CuO/CaO(10 : 90)(ES)(700 °C), and (d) ZnO/CaO(10 : 90)(ES)(700 °C).

modified catalysts around 44.7 to 54.1 wt% due to the higher ratio of CaO (90 wt%) used as a based catalyst. Furthermore, the composition of O was detected to be around 36.6 to 49.5 wt% in all modified catalysts due to the oxide from metal elements on the catalyst surface. For the NiO/CaO(10 : 90)(ES) catalyst calcined at 700 °C, it was noted that the elemental compositions present in this catalyst were 44.7 wt% of Ca, 47.3 wt% of O and 1.8 wt% of Ni. However, after calcination at 800 °C, the weight percentage of the detected Ca, O and Ni in the catalyst increased to 46.8 wt%, 49.5 wt% and 3.8 wt%, respectively. This was possibly due to the growth of catalyst particles, which led to the sintering of a fine crystal when it was exposed to the higher temperature.

Meanwhile, the CuO/CaO(10 : 90)(ES) catalyst calcined at 700 °C showed the elemental composition of Ca (54.1 wt%), O (49.5 wt%) and Cu (9.3 wt%). Apparently, this catalyst consisted of the highest weight percentage of Ca, as compared to other synthesized catalysts. This was supported by the XRD analysis result, in which the CuO-doped CaO (ES) catalyst recorded more peaks related to the copper dopant, which were monoclinic CuO and tetragonal primitive $CaCuO_2$, as well as possess the highest crystallite size of cubic CaO, monoclinic CuO and tetragonal primitive $CaCuO_2$. Next, for the ZnO/CaO(10 : 90)(ES) catalyst calcined at 700 °C, the EDX analysis revealed an elemental composition of 45.8% of Ca, 48.4% of O and 5.8% of Zn. Overall, it was concluded that all of the modified catalysts do not have any impurities or contaminations, as they only consist of the elements Ni, Cu, Zn, Ca and O.

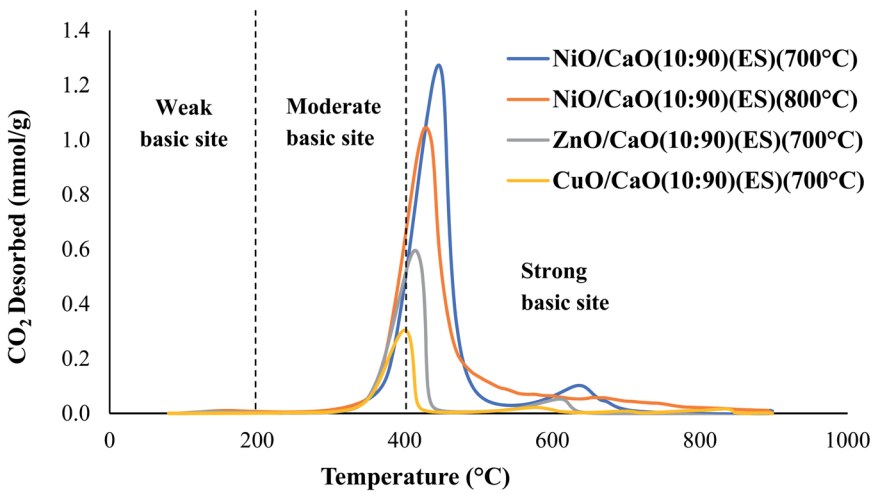

Fig. 8 CO_2-TPD profiles of the NiO/CaO(10 : 90)(ES) catalysts calcined at 700 °C and 800 °C, CuO/CaO(10 : 90)(ES) and ZnO/CaO(10 : 90)(ES) catalysts calcined at 700 °C for 5 hours.

Table 6 The quantity of desorbed peak CO_2 and total basicity over the modified CaO (ES) catalysts

Catalysts	Temperature of desorbed peak CO_2 (°C)	Quantity of desorbed peak CO_2 (mmol g^{-1})	Total basicity (mmol g^{-1})
NiO/CaO(10 : 90)(ES)(700 °C)	438.80	6.9984	8.5867
	639.80	1.5883	
NiO/CaO(10 : 90)(ES)(800 °C)	421.10	6.7964	6.7964
ZnO/CaO(10 : 90)(ES)(700 °C)	412.10	3.1830	3.5911
	607.10	0.4081	
CuO/CaO(10 : 90)(ES)(700 °C)	398.20	1.5387	1.6918
	576.80	0.1531	

3.3.5. CO_2-temperature programmed desorption (CO_2-TPD) analysis. Fig. 8 presents the CO_2-TPD profiles of the NiO/CaO(10 : 90)(ES) catalysts calcined at 700 °C and 800 °C, and the CuO/CaO(10 : 90)(ES) and ZnO/CaO(10 : 90)(ES) catalysts calcined at 700 °C for 5 hours. The CO_2 desorption peaks can be divided into three groups, exhibiting weak basic sites at a temperature ranging from 50 °C to 200 °C that corresponded to the surface hydroxyl groups (OH^-); moderate basic sites at a temperature from 200 °C to 400 °C, which can be attributed to the oxygen of the metal–oxygen ion pairs (Me^+–O^{2-}); and strong basic sites at a temperature between 400 °C and 800 °C, which referred to the isolated surface O^{2-} anions that possess Lewis base character, as explained by Sulaiman *et al.*[29] From the TPD profile shown in Fig. 8, most of the CO_2 desorption peaks exhibited by all catalysts were observed at a temperature above 400 °C that were assigned to strong basic sites. It was observed that only this catalyst possessed two types of basic sites; medium and strong basic sites. The details on the total basicity of each modified catalyst are tabulated in Table 6.

From the data illustrated in Table 6, the calcination temperature and type of dopants affected the basicity of the catalyst. For the NiO/CaO(10 : 90)(ES) catalysts, the result showed that the total basicity decreased with increasing calcination temperature from 8.5867 mmol g^{-1} (700 °C) to 6.7964 mmol g^{-1} (800 °C). As reported by Yan *et al.*,[30] the calcination temperature mostly affects the basicity of the catalyst, surface area and catalytic performance towards the transesterification reaction. As the specific surface area decreased, the basicity was decreased from the amount of exposed basic sites per unit volume. This phenomenon was due to the diminished amount of basic sites, thus reducing the catalytic efficiency in biodiesel production, as suggested by Kamal *et al.*[27]

Compared to other dopants, it was found that the NiO/CaO(10 : 90)(ES)(700 °C) catalyst possessed the highest amount of basic sites of 8.5867 mmol g^{-1}, followed by the ZnO/CaO(10 : 90)(ES)(700 °C) and CuO/CaO(10 : 90)(ES)(700 °C) catalysts with 3.5911 mmol g^{-1} and 1.6918 mmol g^{-1}, respectively. The total basicity of the modified catalysts increases in the order of Cu < Zn < Ni. Therefore, it was proved that the NiO/CaO(10 : 90)(ES)(700 °C) catalyst exhibited excellent catalytic activity with 97.3% of biodiesel production. As explained by Kamal *et al.*,[31] the addition of the nickel species would improve the Lewis basicity of the catalyst and increase the basic strength that could enhance the biodiesel production. Therefore, it can be concluded that the NiO/CaO(10 : 90)(ES) catalyst calcined at 700 °C gave excellent transesterification catalytic efficiency since it has: (i) the best catalytic texture (*i.e.*, the highest surface area and highest pore volume), (ii) the smallest crystallite size of cubic NiO and cubic CaO, (iii) possible porous nature, and (iv) the highest total basicity with strong basic site, as compared to other prepared catalysts.

3.4. Optimization of the process parameters

3.4.1. Catalyst loading. The effect of catalyst loading (2 to 8 wt%) towards the catalytic performance of NiO/CaO(10 : 90)(ES)(700 °C) was examined. The reaction was carried out at the conditions of 65 °C reaction temperature for 60 minutes with a 1 : 18 oil-to-methanol ratio. The reaction temperature was fixed at 65 °C due to the boiling point of methanol as a reactant being 64.7 °C. As studied by Ngadi *et al.*,[32] the percentage conversion increased with increasing temperature up to 65 °C, and slightly dropped with further increment in temperature. As can be seen in Fig. 9, the yield of biodiesel obtained was 81.2% at 2 wt% catalyst loading. This was due to the insufficient amount of catalyst leading to incomplete reaction, as suggested by Niju *et al.*[33] Meanwhile, as the amount of catalyst loading increased to 6 wt%, the percentage of biodiesel yield was maximized (96.9%). This was probably due to a sufficient amount of catalyst with a high surface area obtained by the NiO/CaO(10 : 90)(ES)(700 °C) catalyst, supplied high interaction between oil and methanol molecules to produce the highest biodiesel yield. Moreover, this maximum yield was achieved due to the availability of active

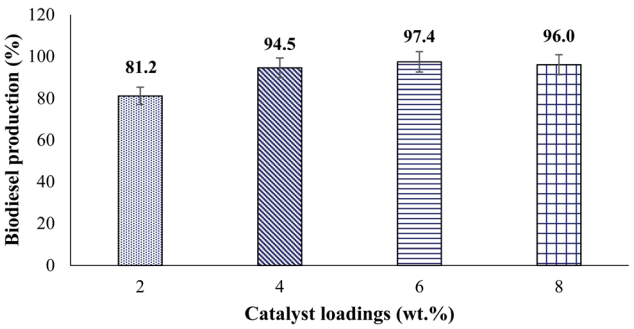

Fig. 9 Percentage of biodiesel production with different catalyst loadings over the NiO/CaO(10 : 90)(ES)(700 °C) catalyst.

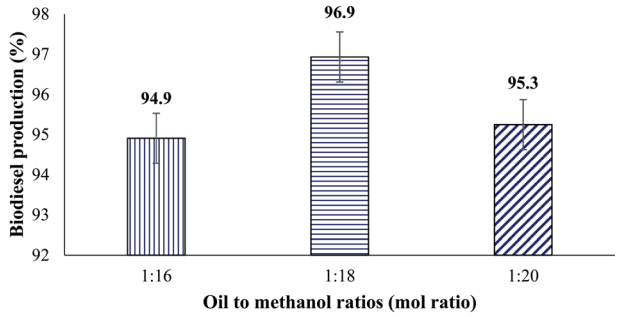

Fig. 10 Percentage of biodiesel production over the NiO/CaO(10 : 90)(ES)(700 °C) catalyst using different oil-to-methanol mol ratios in the transesterification reaction.

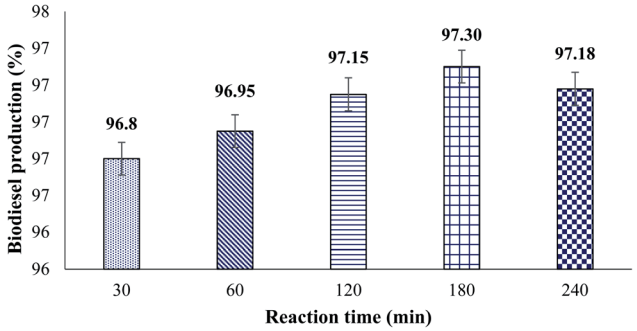

Fig. 11 Percentage of biodiesel production using the NiO/CaO(10 : 90)(ES)(700 °C) catalyst at different reaction times.

sites being increased at the optimum catalyst loading condition in biodiesel production, and this result is in accordance with a study by Arumugam and Sankaranarayanan.[34] However, as the catalyst loading was increased to 8 wt%, the biodiesel yield decreased slightly to 96.0%. This phenomenon was due to the increase in the catalyst loading, which caused the mixture to become too dense and led to reactants and solid catalyst dispersion problems, as stated by Farooq *et al.*[35] Based on this result, 6 wt% of the NiO/CaO(10 : 90)(ES)(700 °C) catalyst loading was selected for further study on the effect of other reaction parameters.

3.4.2. Oil-to-methanol ratio. The effect of the oil-to-methanol ratios (1 : 16, 1 : 18, 1 : 20) in the presence of the NiO/CaO(10 : 90)(ES) catalyst towards biodiesel production was studied. The reaction was conducted at the conditions of 65 °C reaction temperature for 60 minutes with 6 wt% of catalyst loading. Fig. 10 shows that the percentage of biodiesel yield increased as the oil-to-methanol ratio increased. A maximum biodiesel yield of 96.9% was attained by using 1 : 18 of oil-to-methanol ratio. However, beyond this optimum value, the biodiesel yield was slightly decreased to 95.3%. As stated by Taufiq-Yap *et al.*,[36] the separation of biodiesel and glycerol would be difficult due to the excessive addition of methanol, hence affecting the final biodiesel product by shifting the equilibrium in the reverse direction. Moreover, the presence of alcohol in the biodiesel product would have an effect on the fuel quality by reducing its density, viscosity and flash point.[37] Hence, 1 : 18 of oil-to-methanol ratio was selected for the optimization of the reaction time.

3.4.3. Reaction time. In order to examine the effect of the reaction time on the biodiesel yield, the reaction time was varied from 30 to 240 minutes (reaction conditions: 65 °C reaction temperature, 6 wt% catalyst loading and 1 : 18 oil-to-methanol mol ratio), as presented in Fig. 11. The result showed that the biodiesel yield increased with increasing reaction time from 30 to 180 minutes, and subsequently decreased at 240 minutes. This could be due to the biodiesel production being increased in the first stages of the transesterification reaction until it reached equilibrium at 180 minutes, giving the maximum production of 97.30%. However, further increasing the reaction time reduced the biodiesel yield to 97.18%. The reduction of the catalytic performance was probably due to the occurrence of a backward reaction, producing more glycerol than methyl ester, as suggested by Yaşar.[38] Therefore, 180 minutes of reaction time was selected as the optimum reaction time for the transesterification reaction of biodiesel production using the NiO/CaO(10 : 90)(ES) catalyst.

3.4.4. Reusability testing. A catalyst is identified as the best catalyst if it can be reused multiple times by maintaining its efficiency. Reusability testing of the potential catalyst, NiO/CaO(10 : 90)(ES)(700 °C), was carried out to determine the reusability of the catalyst in the transesterification reaction (conditions: 65 °C reaction temperature, 6 wt% catalyst loading, 180 min reaction time and 1 : 18 oil-to-methanol mol ratio). The testing was carried out by repeating the transesterification reaction three times using the used NiO/CaO(10 : 90)(ES)(700 °C) catalyst under optimized conditions. As shown in Fig. 12, the biodiesel production gave 94.4% and 93.4% in the second and third run, respectively. Previous research by Kaur and Ali[39] suggested that the gradual loss in catalytic activity after each run might be caused by the blocking of active sites either due to the organic molecule adsorption or atmospheric O_2, H_2O and CO_2 contamination. In addition, during the catalytic process, the structural changes often deactivate the catalyst and thereby decrease the activity. Overall, it could be seen that after being used for 3 times, the catalyst still yielded more than 93% of the biodiesel production, strongly suggesting high reusability of this potential NiO/CaO(10 : 90)(ES)(700 °C) catalyst. Therefore,

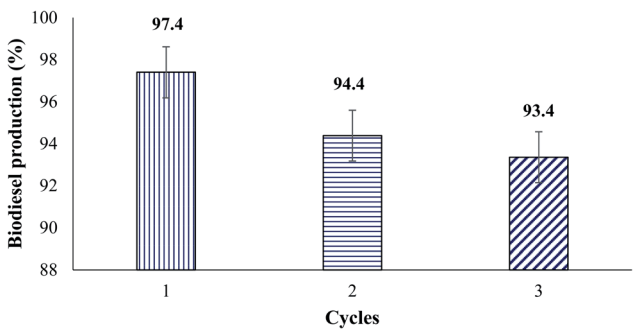

Fig. 12 Reusability testing over the NiO/CaO(10 : 90)(ES)(700 °C) catalyst.

Table 7 ANOVA data of the response surface quadratic model over the NiO/CaO(10 : 90)(ES)(700 °C) catalyzed reaction

Source	Freedom degree	Sum of squares	Mean squares	*F*-value	*p*-value
Model	9	17.59	1.95	5654.05	<0.0001[a]
X_1	1	1.43	1.43	4130.72	<0.0001
X_2	1	1.26	1.26	3656.34	<0.0001
X_3	1	0.024	0.024	70.00	<0.0001
X_1X_2	1	0.0036	0.0036	10.41	0.0145
X_1X_3	1	0.31	0.31	907.11	<0.0001
X_2X_3	1	1.17	1.17	3373.88	<0.0001
X_1^2	1	5.36	5.36	15 496.63	<0.0001
X_2^2	1	5.26	5.26	15 223.08	<0.0001
X_3^2	1	1.48	1.48	4282.81	<0.0001
Residual	7	0.0024	0.0003		
Lack of fit	3	0.0019	0.0006	4.87	0.0801[b]
Pure error	4	0.0005	0.0001		
Total	16	17.59			
Std. Dev.	0.019	R-squared		0.9999	
Mean	95.96	Adj. R-squared		0.9997	
C.V. %	0.019	Pred. R-squared		0.9982	

[a] Significant. [b] Not significant.

the resulting catalyst is proven as an effective solid base catalyst with high reusability.

3.5. Optimization of the NiO/CaO(10 : 90)(ES)(700 °C) catalyzed reaction by RSM

A three-level-three-factor Box–Behnken design was developed to verify the optimization of the NiO/CaO(10 : 90)(ES)(700 °C) catalyzed reaction over the biodiesel production parameters. The model expressed by eqn (5) represents the biodiesel production (Y) as a dependent response towards the catalyst loading (X_1), oil-to-methanol ratio (X_2) and reaction time (X_3). The ANOVA data for the determination of significance on the quadratic model over NiO/CaO(10 : 90)(ES)(700 °C) catalysis is presented in Table 7. The *F*-value for the terms incorporated in the model was 5654.05 with *p*-values < 0.0001, suggesting that the model was significant. As stated by Hassan *et al.*,[40] the *p*-value represents the probability of error in order to verify the significance of each regression coefficient. The main design indicates that the terms significantly affecting the production of biodiesel corresponded to X_1, X_2, X_3 and the relationship between the main factors (X_1X_2, X_1X_3, and X_2X_3), while there were no insignificant quadratic terms (X_1^2, X_2^2, and X_3^2) on biodiesel production. Thus, it was found that the *p*-value of the model was very significant as the *p*-values were less than 0.05.

$$Y = 97.30 + 0.42 \times X_1 + 0.40 \times X_2 + 0.055 \times C - 0.03 \times X_1 \times X_2 - 0.28 \times X_1 \times X_3 + 0.54 \times X_2 \times X_3 - 1.13 \times X_1^2 - 1.12 \times X_2^2 - 0.59 \times X_3^2 \quad (5)$$

Moreover, the *p*-value of the lack-of-fit test for the NiO/CaO(10 : 90)(ES)(700 °C) catalyzed reaction was found to be 0.0801, which verified that the model was acceptable for experimental results. Moreover, a lower number of coefficient variation (CV, 0.019%) indicates the high accuracy and reliability of the experimental values in the reaction models. The fit of the developed regression equation could be measured by the determination coefficient (R^2), which was 0.9999. The predicted R^2 value of 0.9982 corresponded to the adjusted R^2 value of 0.9997, indicating that the data matched well with the model, and the results were convincingly good in their range. From the ANOVA data, it can be inferred that the most important parameter was the catalyst loading, which had a *F*-value of 4130.72, followed by the oil-to-methanol ratio (3656.34) and reaction time (70.00).

The effects of the catalyst loading and oil-to-methanol ratio towards biodiesel production over the NiO/CaO(10 : 90)(ES)(700 °C) catalyzed reaction are depicted in 3D and 2D contour plots (Fig. 13(a)). The reaction time was kept constant at 180 minutes. The red point in the middle of the surface plot showed the designed center point, indicating five times replication and the designed space were in a good predictability. The production of biodiesel increased until the maximum production was reached with increasing oil-to-methanol ratio and catalyst loading. As the oil-to-methanol ratio and catalyst loading reached a high level, the biodiesel production was moderately decreased. It can be inferred that the reaction achieved an equilibrium at optimum conditions and shifted to a reverse reaction.

Moreover, Fig. 13(b) shows the interaction of the reaction time and catalyst loading on biodiesel production, while the oil-to-methanol mol ratio was fixed at 1 : 18. The increased reaction time and catalyst loading contributed to the maximum production of biodiesel. Fig. 13(c) also illustrates the impact on biodiesel production over the reaction time and oil-to-methanol ratio, while the catalyst loading remained constant at 6 wt%. It was observed that the production of biodiesel increased to more than 97% with a 1 : 18 oil-to-methanol ratio at 180 minutes. Thus, the interaction from the elliptical contour plots displayed in

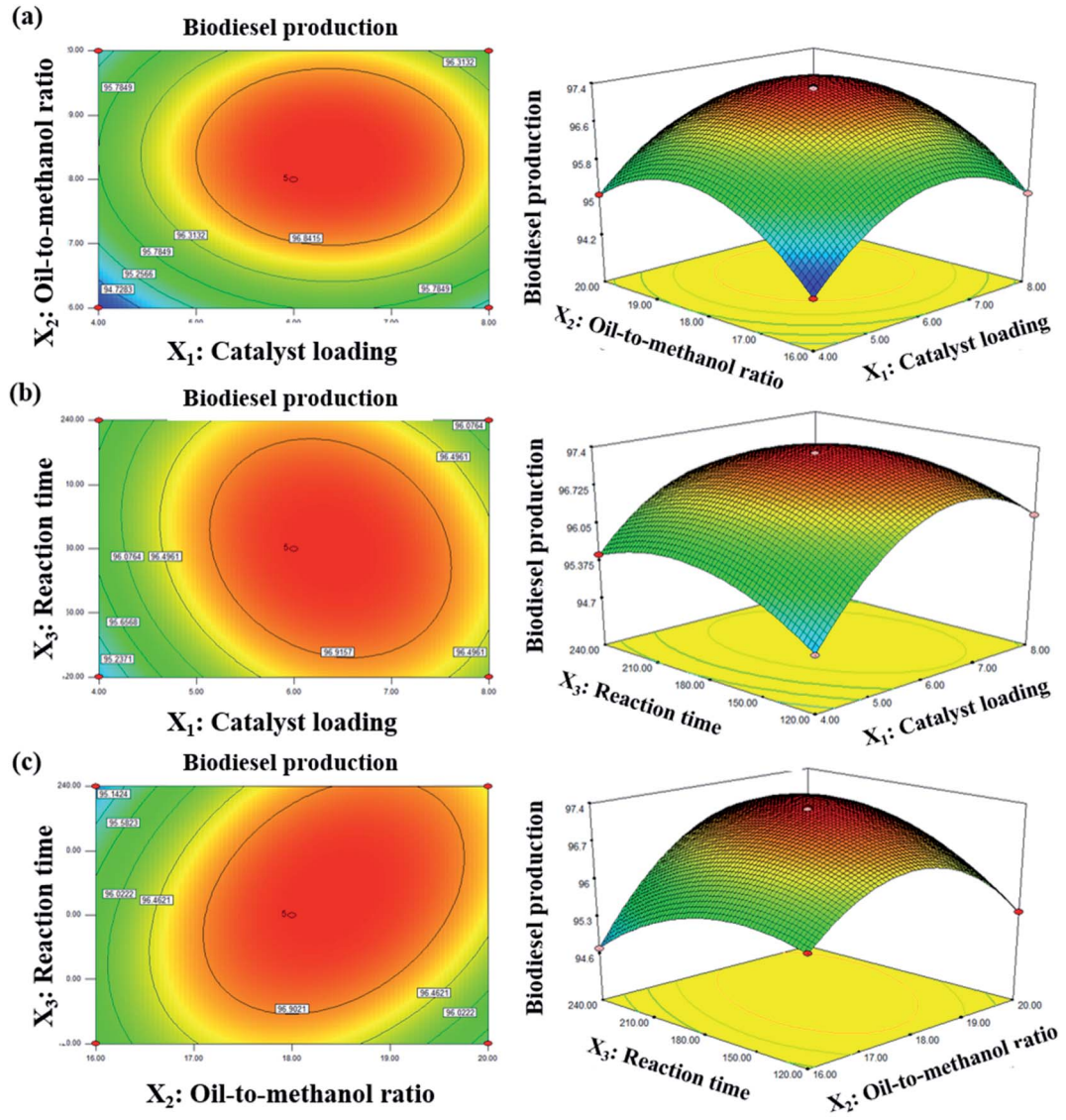

Fig. 13 3D surface plots and 2D contour plots of the NiO/CaO(10 : 90)(ES)(700 °C) catalyzed reaction as a function of the (a) oil-to-methanol ratio and catalyst loading, (b) reaction time and catalyst loading, and (c) reaction time and oil-to-methanol ratio.

Fig. 13 for these three independents factors in biodiesel production was significant and successful.

The optimum design conditions were identical to the experimental findings. The experimental results achieved 97.3% of maximum biodiesel production, while the predicted biodiesel yield was estimated at 97.3%. Therefore, as the experimental and predicted values were closely aligned, the model is highly recommended and reliable for producing biodiesel from refined waste cooking oil.

4. Conclusion

New heterogenous catalysts for the transesterification of the NiO, CuO and ZnO-modified CaO-based catalysts derived from waste shell were successfully synthesized *via* wetness impregnation method. The catalytic testing results demonstrated that the NiO/CaO(10 : 90)(ES) catalyst, which was calcined at 700 °C, appeared as the catalyst with the most potential for the transesterification of refined waste cooking oil. The optimization over the NiO/CaO(10 : 90)(ES) catalyzed reaction was verified by RSM using the Box–Behnken design. It was found that the NiO/CaO(10 : 90)(ES)(700 °C) catalyst showed the highest activity (97.3%) at the optimum reaction conditions of 65 °C of reaction temperature, 6 wt% of catalyst loading, 1 : 18 of oil-to-methanol molar ratio, and 180 minutes of reaction time. Characterizations suggested that the relatively high surface area of 7.1 m^2 g^{-1} and basicity of 8.5867 mmol g^{-1} both contributed to the excellent catalytic activity of the NiO/CaO(10 : 90)(ES)(700 °C) catalyst. The research findings indicated that the acid value and free fatty acids of the biodiesel produced from refined cooking oil using the synthesized NiO modified CaO catalyst at optimal process conditions followed the EN 14214 and ASTM D6751 limit with 0.17 mg KOH per g (AV) and 0.09 mg KOH per g (FFA), respectively. The NiO/

CaO(10 : 90)(ES)(700 °C) catalyst showed good reusability for 3 consecutive reaction cycles.

Author contributions

Nur Fatin Sulaiman: conceptualization, writing – original draft, methodology, software, formal analysis, supervision; Nurul Izzaty Ramly: writing – original draft, methodology, resources, validation; Mohamad Helmi Abd Mubin: conceptualization, software; and Siew Ling Lee: supervision, funding acquisition, resources, investigation, writing – review and editing.

Conflicts of interest

There are no conflicts to declare.

Acknowledgements

The authors are grateful to the Ministry of Education (MOE), Malaysia and Universiti Teknologi Malaysia (UTM) for the financial support given under UTM High Impact Research Grant (Cost Center No. Q. J130000.2454.08G53), and PDRU Grant Vote No. 04E70 to N. F. Sulaiman.

References

1 M. B. Vieira, D. M. B. Costa, T. M. Mata, A. A. Martins, M. A. V. Freitas and N. S. Caetano, Environmental assessment of industrial production of microalgal biodiesel in central-south Chile, *J. Cleaner Prod.*, 2020, **266**, 121756.

2 W. Roschat, S. Phewphong, A. Thangthong, P. Moonsin, B. Yoosuk, T. Kaewpuang and V. Promarak, Catalytic performance enhancement of CaO by hydration-dehydration process for biodiesel production at room temperature, *Energy Convers. Manage.*, 2018, **165**(2), 1–7.

3 J. M. Cerveró, J. R. Álvarez and S. Luque, Novozym 435-catalyzed synthesis of fatty acid ethyl esters from soybean oil for biodiesel production, *Biomass Bioenergy*, 2014, **61**(3), 131–137.

4 A. Galadima and O. Muraza, Waste materials for production of biodiesel catalysts: Technological status and prospects, *J. Cleaner Prod.*, 2020, **263**, 121358.

5 M. Catarino, M. Ramos, A. P. Soares Dias, M. T. Santos, J. F. Puna and J. F. Gomes, Calcium rich food wastes based catalysts for biodiesel production, *Waste Biomass Valorization*, 2017, **8**, 1699–1707.

6 L. J. Konwar, J. Boro and D. Deka, Review on latest developments in biodiesel production using carbon-based catalysts, *Renewable Sustainable Energy Rev.*, 2014, **29**(3), 546–564.

7 S. I. Wilkanowicz, N. R. Hollingsworth, K. Saud, U. Kadiyala and R. G. Larson, Immobilization of calcium oxide onto polyacrylonitrile (PAN) fibers as a heterogeneous catalyst for biodiesel production, *Fuel Process. Technol.*, 2020, **197**, 106214.

8 G. Baskar and R. Aiswarya, Trends in catalytic production of biodiesel from various feedstocks, *Renewable Sustainable Energy Rev.*, 2016, **57**(4), 496–504.

9 A. Navajas, T. Issariyakul, G. Arzamendi, L. M. Gandía and A. Dalai, Development of eggshell derived catalyst for transesterification of used cooking oil for biodiesel production, *Asia-Pac. J. Chem. Eng.*, 2013, **8**(5), 742–748.

10 N. Mansir, S. H. Teo, U. Rashid, M. I. Saiman, Y. P. Tan, G. A. Alsultan and Y. H. T. Yap, Modified waste egg shell derived bifunctional catalyst for biodiesel production from high FFA waste cooking oil. A review, *Renewable Sustainable Energy Rev.*, 2018, **82**, 3645–3655.

11 S. Kaewdaeng, P. Sintuya and R. Nirunsin, Biodiesel production using calcium oxide from river snail shell ash as catalyst, *Energy Procedia*, 2017, **138**(5), 937–942.

12 N. Mijan, Synthesis and catalytic activity of hydration–dehydration treated clamshell derived CaO for biodiesel production, *Chem. Eng. Res. Des.*, 2015, **102**(7), 368–377.

13 A. P. S. Chouhan and A. K. Sarma, Modern heterogeneous catalysts for biodiesel production: A comprehensive review, *Renewable Sustainable Energy Rev.*, 2011, **15**(9), 4378–4399.

14 S. J. Yoo, H. S. Lee, B. Veriansyah, J. Kim, J. D. Kim and Y. W. Lee, Synthesis of biodiesel from rapeseed oil using supercritical methanol with metal oxide catalysts, *Bioresour. Technol.*, 2010, **101**, 8686–8689.

15 S. Dawood, A. K. Koyande, M. Ahmad, M. Mubashir, S. Asif, J. J. Klemes, A. Bokhari, S. Saqib, M. Lee, M. A. Qyyum and P. L. Show, Synthesis of biodiesel from non-edible (Brachychiton populneus) oil in the presence of nickel oxide nanocatalyst: Parametric and optimisation studies, *Chemosphere*, 2021, **278**, 130469.

16 V. Gayakhe, S. Bhilare, A. Yashmeen, I. J. S. Fairlamb and A. R. Kapdi, Chapter 6 - Transition-Metal Catalyzed Modification of Nucleosides, *Palladium-Catal. Modif. Nucleosides, Nucleotides Oligonucleotides*, 2018, **58**(11), 167–195.

17 N. F. Sulaiman, W. A. Wan Abu Bakar and R. Ali, Response surface methodology for the optimum production of biodiesel over Cr/Ca/γ-Al_2O_3 catalyst: Catalytic performance and physicochemical studies, *Renewable Energy*, 2017, **113**(3), 697–705.

18 P. Kowalik and W. Próchniak, The effect of calcination temperature on properties and activity of Cu/ZnO/Al2O3 catalysts, *Annales UMCS, Chemistry*, 2010, **65**(4), 79–87.

19 J. Yan, G. Wu, N. Guan, L. Li, X. Li and X. Cao, Understanding the effect of surface/bulk defects on the photocatalytic activity of TiO_2: Anatase *versus* rutile, *Phys. Chem. Chem. Phys.*, 2013, **15**(26), 10978–10988.

20 Q. Fu and X. Bao, Catalysis on a metal surface with a graphitic cover, *Chin. J. Catal.*, 2015, **36**, 517–519.

21 N. F. Sulaiman, W. A. W. A. Bakar, S. Toemen, N. M. Kamal and R. Nadarajan, In depth investigation of bi-functional, Cu/Zn/γ-Al_2O_3 catalyst in biodiesel production from low-grade cooking oil: Optimization using response surface methodology, *Renewable Energy*, 2019, **135**(17), 408–416.

22 N. F. Sulaiman, S. L. Lee and A. R. Yacob, Transesterification reaction from rice bran oil to biodiesel over heterogeneous

base calcium oxide nanoparticles catalyst, *Science and Technology Indonesia*, 2020, **5**(3), 62–69.

23 J. A. Melero, L. F. Bautista, G. Morales, J. Iglesias and R. S. Vazquez, Acid-catalyzed production of biodiesel over arenesulfonic SBA-15: Insights into the role of water in the reaction network, *Renewable Energy*, 2015, **75**, 425–432.

24 R. B. Ljupković, R. D. Mićić, M. D. Tomić, N. S. Radulović, A. L. Bojić and A. R. Zarubica, Significance of the structural properties of CaO catalyst in the production of biodiesel: An effect on the reduction of greenhouse gas emissions, *Hem. Ind.*, 2014, **68**(4), 399–412.

25 T. Roy, S. Sahani, D. Madhu and Y. C. Sharma, A clean approach of biodiesel production from waste cooking oil by using single phase $BaSnO_3$ as solid base catalyst: Mechanism, kinetics & E-study, *J. Cleaner Prod.*, 2020, **265**, 121440.

26 A. Rownaghi, Y. H. Taufiq-Yap and F. Rezaei, Solvothermal synthesis of vanadium phosphate catalysts for n-butane oxidation, *Chem. Eng. J.*, 2009, **155**(2), 514–522.

27 N. H. Kamal, W. A. W. A. Bakar and R. Ali, Catalytic optimization and physicochemical studies over Zn/Ca/Al_2O_3 catalyst for transesterification of low grade cooking oil, *Energy Convers. Manage.*, 2017, **137**(5), 113–120.

28 S. Niju, K. M. M. S. Begum and N. Anantharaman, Enhancement of biodiesel synthesis over highly active CaO derived from natural white bivalve clam shell, *Arabian J. Chem.*, 2016, **9**, 633–639.

29 N. F. Sulaiman, S. L. Lee, S. Toemen and W. A. W. A. Bakar, Physicochemical characteristics of Cu/Zn/γ-Al_2O_3 catalyst and its mechanistic study in transesterification for biodiesel production, *Renewable Energy*, 2020, **156**, 142–157.

30 S. Yan, M. Kim, S. Mohan, S. O. Salley and K. Y. S. Ng, Effects of preparative parameters on the structure and performance of Ca–La metal oxide catalysts for oil transesterification, *Appl. Catal., A*, 2010, **373**(1), 104–111.

31 N. H. Kamal, W. A. W. A. Bakar, S. Toemen and R. Ali, Biodiesel production *via* transesterification of low grade cooking oil over heterostructure nano particles of Ni/Mg/Al_2O_3 catalyst, *Int. J. Eng., Trans. B*, 2018, **31**(3), 1318–1325.

32 N. Ngadi, S. Sulaiman, R. Rahman and N. Lani, Production of biodiesel from palm oil using cockle shell waste as heterogeneous catalyst, *J. Teknol.*, 2017, **79**(3), 145–154.

33 S. Niju, K. M. Meera, S. Begum and N. Anantharaman, Modification of egg shell and its application in biodiesel production, *J. Saudi Chem. Soc.*, 2014, **18**(5), 702–706.

34 A. Arumugam and P. Sankaranarayanan, Biodiesel production and parameter optimization: An approach to utilize residual ash from sugarcane leaf, a novel heterogeneous catalyst, from *Calophyllum inophyllum* oil, *Renewable Energy*, 2020, **153**, 1272–1282.

35 M. Farooq, A. Ramli and A. Naeem, Biodiesel production from low FFA waste cooking oil using heterogeneous catalyst derived from chicken bones, *Renewable Energy*, 2015, **76**(2), 362–368.

36 Y. H. Taufiq-Yap, H. Lee and P. L. Lau, Transesterification of *jatropha curcas* oil to biodiesel by using short necked clam (*orbicularia orbiculata*) shell derived catalyst, *Energy Explor. Exploit.*, 2012, **30**(9), 853–866.

37 T. A. Degfie, T. T. Mamo and Y. S. Mekonnen, Optimized biodiesel production from waste cooking oil (WCO) using calcium oxide (CaO) nano-catalyst, *Sci. Rep.*, 2019, **9**(1), 18982–18994.

38 F. Yaşar, Utilization of waste eggshell as catalyst in biodiesel production and investigation of efficiency, density and viscosity parameters of biodiesel obtained in different reaction times, *International Journal of Automotive Engineering and Technologies*, 2019, **8**(5), 22–28.

39 N. Kaur and A. Ali, Kinetics and reusability of Zr/CaO as heterogeneous catalyst for the ethanolysis and methanolysis of *Jatropha crucas* oil, *Fuel Process. Technol.*, 2014, **119**(11), 173–184.

40 A. A. Hassan, H. A. Alhameedi and J. D. Smith, Using ethanol for continuous biodiesel production with trace catalyst and CO_2 co-solvent, *Fuel Process. Technol.*, 2020, **23**, 106377.